CUURENT STATUS OF DEBRIS PROTECTION DESIGN STANDARD AT JAXA

Kumi Nitta[(1)],
JAXA DESIGN STANDARD Micro-debris Impact Survivability Assessment Procedure WG

[(1)] 1 Safety and Mission Assurance Department Japan Aerospace Exploration Agency (JAXA)
2-1-1 Sengen, Tsukuba-shi, Ibaraki 305-8505JAPAN, nitta.kumi@jaxa.jp:

ABSTRACT

We have been conducting hypervelocity impact tests and numerical simulations in order to create Japanese design guidelines that protect satellites against a certain degree of impact by micrometeoroids and orbital debris (hereinafter referred to as M/OD). Certain members of JAXA, university researchers, computer analysts, and spacecraft manufacturers formed a working group to investigate the impact effect of OD on critical parts and bumpers, by conducting hypervelocity impact (HVI) tests and analysis. The knowledge acquired is now being reflected in spacecraft design.

We plan to continue and extend our experimental and numerical investigations covering a wider and more diverse range of conditions, to complete the guidelines at JAXA for the purpose of protecting unmanned spacecraft against impacts from space debris and micrometeoroids.

1 INTRODACTION

The "Midori II" satellite (also known by its development codename "ADEOS II") was launched by Japan in 2002, but its operation was ended prematurely in 2003 by a solar panel malfunction. This failure was putatively due to electrostatic charge/discharge (ESD), and one of the causes was presumed to be damage to electrical power cables by the impact of micrometeoroids and space debris (M/OD) [1][2][3], since the power carried by the cables was consistent with the loss of generated power on the satellite. The investigation of the failure causes, and efforts to determine future countermeasures, indicated that enhanced ground tests and verification under as realistic a space environment as possible are necessary. One measure has been to create a Japanese design standard for protecting satellites from M/OD impacts, and we have been contributing to this effort by conducting hypervelocity impact tests and numerical simulations. We try to investigate the simulation results agreed with experiments under the same conditions. This requires an investigation that starts over from fundamentals, beginning with the parameter of various material and condition. The purpose of this study was to create the assessment procedure for verifying the validity of the protection design of satellites and probes (hereinafter referred to as spacecraft) against risks of impact with micro debris and meteoroid (hereinafter referred to as debris) which are 1 mm or less in size and whose impact probability and impact damage is not negligible.

2 CONDITION FOR ASSESSMENT

We introduce this standard describes the assessment procedure for verifying the validity of the protection design of satellites and probes (hereinafter referred to as spacecraft) against risks of impact with M/OD which are 1 mm or less in size and whose impact probability and impact damage is not negligible.

To ensure the spacecraft mission in the environment of the micro-debris and meteoroid, the following points including the system design must be coordinated during the progress of the development of the system from the Mission Requirements Definition Phase.

(1) Consideration of debris density when determine the operational orbit altitude

(2) Consideration of the distribution of debris impact probability when determine the shape of spacecraft.

(3) Setting the policy concerning the allowable limit of impact risk (mission importance, relationship with other redundant elements, etc.)

(4) Assessment in view of system design including the influence of loss of mass and layout change of components associated with impact protection measures (including allocation of resources)

(5) Setting a contingency plan including impact detection, damage monitoring, recovering, reconstruction and isolation

This standard serves as guidance for impact protection design on the condition that the spacecraft has been defined in shape, dimensions, operational orbital characteristics, and operational period considering above conditions.

From the numerical analysis shown in Section 3 and the mutual verification of the experiment and numerical analysis shown in Section 4, we derived a ballistic limit

Proc. 8th European Conference on Space Debris (virtual), Darmstadt, Germany, 20–23 April 2021, published by the ESA Space Debris Office
Ed. T. Flohrer, S. Lemmens & F. Schmitz, (http://conference.sdo.esoc.esa.int, May 2021)

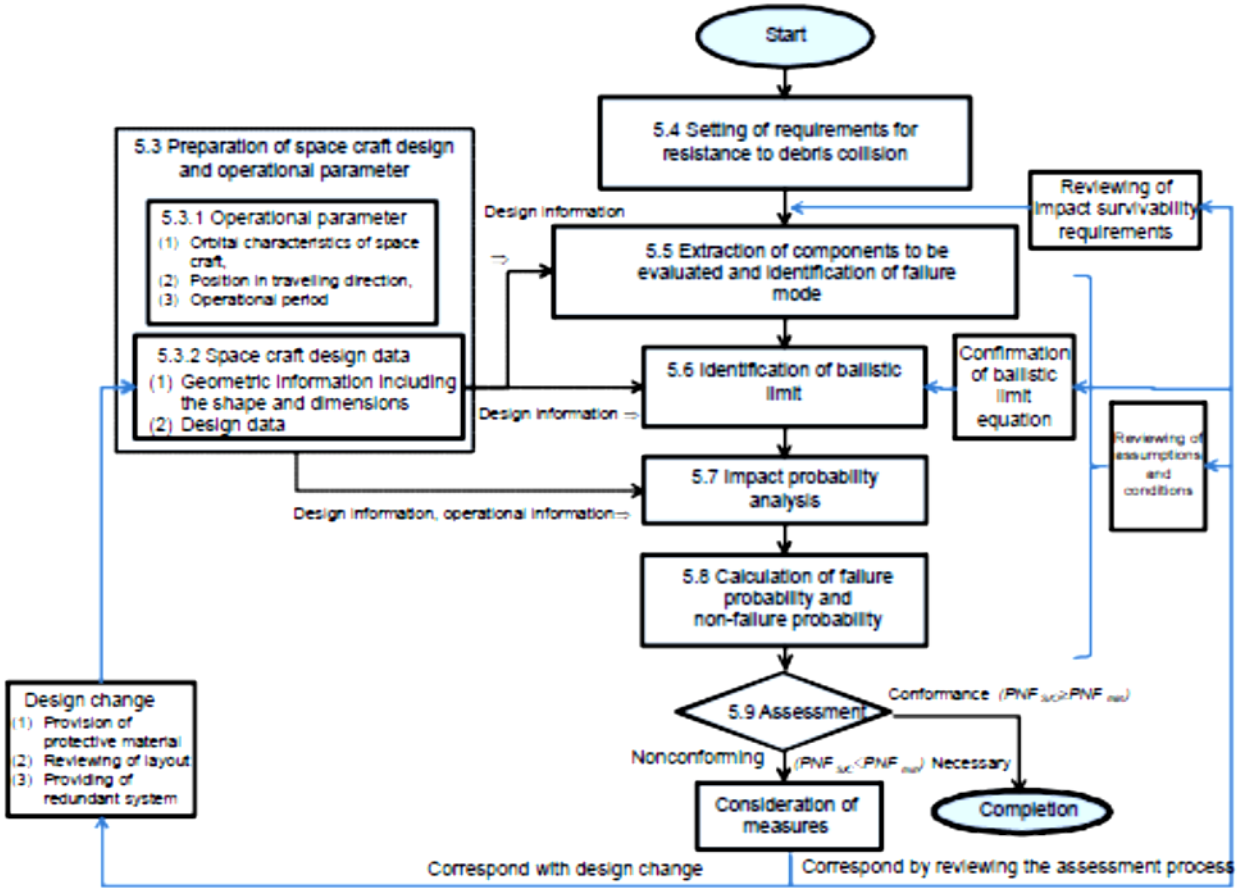

Figure 1 Assessment flow diagram

～2014 Establishment of numerical analysis method for basic structure	2015～2017 Acquisition of ballistic limit curve required for protective design	2018～ (TBD) Organize the results and decide the future direction
Established the following analysis method ・Aluminum plate ・Honeycomb sandwich structure ・Power harness ・Aramid fiber woven fabric The following ballistic limit curve was acquired, and the validity of the data was confirmed. ・Aluminum plate ・Honeycomb sandwich structure ・Power harness ・Aramid fiber woven fabric	The following ballistic limit curve was acquired ・Protection of harness bundles with woven fabric ・Protection of harness bundle with aluminum plate ・Gap in the power harness bundle (Considering evaluation method) ・CFRP skin Honeycomb sandwich structure ・aluminum skin Honeycomb sandwich structure ・Aluminum plate protected by aluminum plate	Matters to be considered (draft) ・Aluminum plate protected by aluminum plate (Additional defense aluminum plate thickness) ・CFRP skin Honeycomb sandwich structure（Additional skin material） ・Aluminum plate behind the honeycomb panel ・Diagonal collision with honeycomb panel ・Protection of harness bundle with aluminum plate（Addition of thickness variety） ・Gap in the power harness bundle ・Honeycomb panel behind the harness

F

figure 2 Implementation plan.

curve that can be used for the combination of structures and protective materials, which is highly requested by spacecraft manufacturers.

3 NUMERICAL ANALYSIS METHOD

- **material model**

3.1 Hydrocode

Numerical simulations were performed using the ANSYS AUTODYN hydrocode. As in almost all hydrocodes, the material model in ANSYS AUTODYN consists of three parts: i) an equation of state (E.O.S.) describing the relationships between pressure, density and internal energy (not temperature), ii) a material strength model that expresses constitutive relations of solid materials, and iii) a failure or fracture model. While a failure model for solid materials is typically used, the model can also incorporate spalling (fracture by negative pressure) of liquid materials. In spite of their name, therefore, hydrocodes are formulated to simulate the highly dynamic and non-linear behaviours of materials not only in the liquid phase but also in the solid and gas phases, and sometimes even the plasma state can be simulated approximately by use of an appropriate E.O.S.

3.2 Projectile

Orbital space debris is composed of artificial objects which have been created through human space activities in near-Earth space since the launch of Sputnik I. The average density of space debris is considered to be 2.8–4.7 g/cm3 for objects smaller than 10 mm, while the relative impact velocity of orbital space debris in low earth orbit (LEO) is theoretically limited to approximately 16 km/s. In this assessment, the space debris material is assumed to be aluminium alloy, SS304 or alumina. The propellant used in solid rocket motors (SRM) contains about 18% aluminium by weight, and these motors eject alumina particles that range in size from μm-order dust up to cm-order slugs into earth orbit.

In our study, comparison of simulation results with corresponding experiments led to the selection of the Steinberg-Guinan strength model [4] for stainless steels. The material model includes an equation of state (“pressure”), a constitutive (“strength”) model and a fracture or failure (“damage”) model.

3.3 Targets

The targets experimentally tested and simulated numerically in this assessment are a 0.35 mm-thick sheet of harness cable coating material, a 1 mm thick sheet of ETFE, and a 5 mm-thick 2024-T3 aluminium alloy panel. The Tillotson equation of state [5] was applied to materials that would be subjected to extreme physical conditions because it takes into account shock-induced vaporization. The Steinberg–Guinan strength model [4] was applied to ductile materials (in this case, the aluminium alloy).

4 EXPERIMENTAL FACILITIES

A series of experiments were carried out using a two-stage light-gas gun at an ISAS/JAXA facility, shown in Fig. 2, which can accelerate a 0.2 g projectile up to 7 km/s. The spherical projectiles are initially covered with a cylindrical polycarbonate sabot with a diameter of 7.1 mm and a length of 10.5 mm, which guides the projectiles in the helium driving gas during acceleration and detaches after sufficient velocity is attained. The projectiles impact a target in a test chamber evacuated to a pressure of around 0.1 Pa.

Test results are compared with corresponding simulation results and discussed from the viewpoint of assessing protection of satellites against M/OD hypervelocity impacts. The material models used in the numerical simulations that enable the assessment of phenomena corresponding to a wide range of impact velocities, including shock-induced vaporization, are also discussed. The accuracy of the numerical simulations was validated by comparing the computed results with gas gun experiments.

Figure 3. Two-stage light-gas gun at ISAS/JAXA

5 INPUT STATUS TO DESIGN STANDARDS

After confirming the certainty of the numerical analysis by mutual verification with the experimental results, a parameter study by the numerical analysis is carried out to obtain the Ballistic limit curve. Based on the plan shown in Fig. 2, each configuration is clearly indicated, and the Ballistic limit curve is continuously

published in the design standard handbook [6].

An example of the numerical analysis and experimental results we are conducting is shown in this chapter. Modelled as a disc of sufficient size, the target is an aluminium honeycomb core composed of cells measuring 6.35 mm (1/4 inch) in height and arranged in a regular hexagonal grid as shown in Fig. 4, sandwiched between aluminium skin sheets. Figure 5 depicts the numerical results using Lagrange that simulate the test case shown in Fig. 4. In the experiments using projectiles over 0.3 mm in diameter, damage produced by impact of the fragment cloud was observed on the back-face sheet and surface of the aluminium alloy plate, as shown in Fig. 5. The projectile was considered to have been changed into the fragment cloud by the impact on the front face sheet. The honeycomb core acted similarly to the standoff of a double-wall bumper shield and dispersed the impact energy of the projectiles.

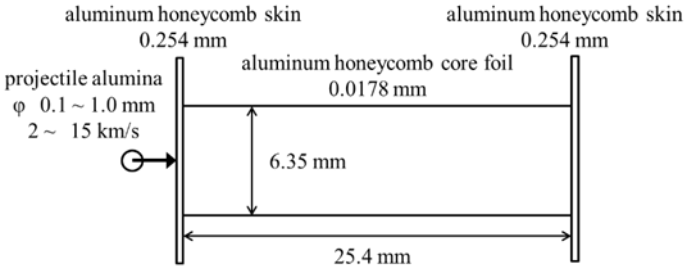

Figure 4 Two-dimensional axial symmetry analytical model of Aluminium honeycomb [7]

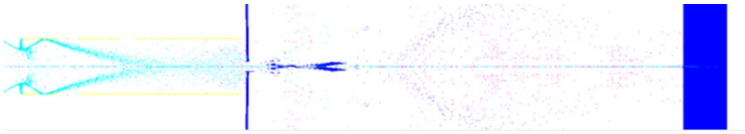

Figure 5 Deformation diagram of calculation results using Lagrange and fragment phenomena at 50 μs, impact velocity of 6 km/s [7]

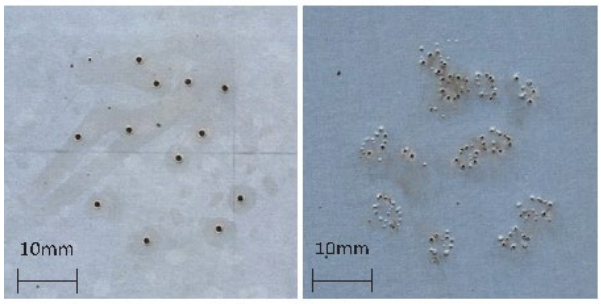

Figure 6 Experimental results of Honeycomb sandwich panel impacted by D = 0.3 mm projectiles at 5.92 km/s: (left) front face sheet, (right) back face sheet [8]

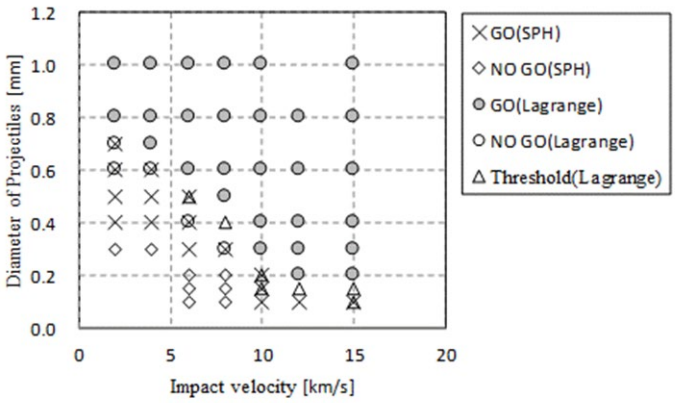

Figure 7. Summary of the numerical simulation results of Honeycomb sandwich panel [7]

Figure 7 shows the ballistic limit of the aluminium honeycomb panel. NO GO, Threshold, and GO denote no penetration to the second skin, a borderline score for penetration, and penetration to the second skin, respectively. As the impact velocity increases, the ballistic limit of the aluminium honeycomb sandwich panel become progressively smaller. This behaviour differs from the ballistic limit curve of a Whipple shield. The ballistic limit of the aluminium honeycomb sandwich panel has a flexion point at an impact velocity of approximately 10 km/s. Our comparison shows that the aluminium honeycomb core negates the beneficial "bumper" effect of two skins. Usually, the projectiles perforated the front face sheet of the honeycomb sandwich panel. When only one projectile impacted a cell, there was no perforation hole on the back-face sheet. Perforated holes on the back-face sheets were only generated in the area under the impacted cells. The foils of cells adjacent to those impacted were damaged, but the fragments did not perforate the back-face sheet under the adjacent cell. This result shows that, in only the impacted cell, the fragments kept sufficient energy to perforate the face sheet and that the honeycomb foils acted as bumpers for the fragment cloud.

The results of numerical simulations adopting these material models were compared with hypervelocity impact tests using a two-stage light-gas gun, and examples of the impacts on an aluminium honeycomb panel were shown. We will continue to extend our experimental and numerical investigations to cover a wider range of conditions, to complete the guidelines for the protection of unmanned spacecraft against space debris and micrometeoroid impacts.

6 ACKNOWLEDGEMENTS

These experiments were conducted and supported by the Space Plasma Laboratory, ISAS, and JAXA. This research was also supported by the JAXA design guideline Working Group 3.

7 REFERENCES

7.1 References

1. Kawakita, S., et al.: Sustained Arc Between Primary Power Cables of a Satellite, AIAA Paper 2004-5658, 2004..

2. Kawakita, S., et al.: Discharge of Spacecraft Solar Panels by Hypervelocity Impact, Transactions of Space Technology Japan, Volume 7, Issue ists26 , 2009, pp. Tr_2_53-Tr_2_56.

3. Nitta, K., et al.: Response of Cable Harness Subjected to High Velocity Impact, Transactions of the Japanese Society for Artificial Intelligence, Aerospace Technology Japan, Volume 8, pp. Pr_2_55-Pr_2_62 ,2012.

4. D.J. Steinberg, S.G. Cochran, M.W. Guinan: A constitutive model for metals applicable at high-strain rate, J. Appl. Phys. 51 pp.1498–1504, 1980

5. J.H. Tillotson: Metallic equations of state for hypervelocity impact. GA-3216, General Atomic, CA, July 1962.

6. JERG-002-144 & Handbook.

7. Investigation on Response of an Aluminum Honeycomb Subjected to Hypervelocity Impacts using Lagrange and SPH for Numerical Modeling Kumi Nitta, Masumi Higashide, Mirai Sueki, Atushi Takeba 2019 15th Hypervelocity Impact Symposium ,2020

8. M. Higashide, N. Onose, and S. Hasegawa, Evaluation of Space Debris Impact on Spacecraft Panels, 2011-r-28, ISTS28th, 2011.